ARTICLE

Symmetry-breaking bifurcations in two mutually delay-coupled lasers

Juancho A. Collera*

Department of Mathematics and Computer Science,
University of the Philippines Baguio

Abstract—We consider a symmetric system of delay differential equations arising from a model of two mutually delay-coupled semiconductor lasers. The system is described using the Lang-Kobayashi rate equations whose basic solutions are called compound laser modes (CLMs). We employ a group-theoretic approach to find solutions and to identify symmetry-breaking steady-state and Hopf bifurcations. This classification allows us to predict the symmetry group of a bifurcating branch of solutions from a symmetry-breaking bifurcation. Methods and techniques used in this study can be extended to larger symmetric laser networks.

Keywords—Symmetry-Breaking Bifurcations, Delay Differential Equations, Delay-Coupled Lasers, Lang-Kobayashi Equations, Equivariant Systems

INTRODUCTION

A pioneering study on the influences of external optical feedback on semiconductor laser properties was done by Lang and Kobayashi (1980). A single mode laser was examined where a portion of the laser output is reflected back to the laser cavity from an external mirror. In dimensionless form, the so-called *Lang-Kobayashi (LK) rate equations* are given by

$$\begin{aligned} \dot{E}(t) &= (1+i\alpha)N(t)E(t)+\kappa e^{-iC_p}E(t-\tau), \\ T\dot{N}(t) &= P-N(t)-(1+2N(t))\,|E(t)|^2, \end{aligned} \tag{1}$$

where $E(t)$ is the complex electrical field and $N(t)$ is the excess carrier number. The parameters α, κ, τ, C_p, T, and P correspond to the linewidth enhancement factor, coupling strength, coupling time, coupling phase, electron decay rate, and pump parameter, respectively. System (1), obtained in Alsing et al. (1996), was reported to accurately describe the dominant effects observed experimentally through computer simulations.

A model of two mutually delay-coupled semiconductor lasers in a face-to-face configuration was studied in Erzgraber et al. (2006) using the following LK-type rate equations:

$$\begin{aligned} \dot{E}_1(t) &= (1+i\alpha)N_1(t)E_1(t)+\kappa e^{-iC_p}E_2(t-\tau)-i\Delta E_1(t), \\ \dot{E}_2(t) &= (1+i\alpha)N_2(t)E_2(t)+\kappa e^{-iC_p}E_1(t-\tau)+i\Delta E_2(t), \\ T\dot{N}_1(t) &= P-N_1(t)-(1+2N_1(t))\,|E_1(t)|^2, \\ T\dot{N}_2(t) &= P-N_2(t)-(1+2N_2(t))\,|E_2(t)|^2, \end{aligned} \tag{2}$$

***Corresponding Author**
Email Address: jacollera@up.edu.ph
Submitted: May 2, 2013
Revised: September 16, 2014
Accepted: February 16, 2015
Published: April 19, 2015
Editor-in-Charge: Jose Maria P. Balmaceda

for complex optical fields $E_1(t)$ and $E_2(t)$, and inversions $N_1(t)$ and $N_2(t)$. Here, the two lasers are coupled via their optical fields, and the time delay τ is the travel time of light to reach the other laser. System (2) is in fact an extension of the LK equations in (1) into the case of two delay-coupled lasers. The detuning parameter Δ measures the difference between optical frequencies of the two uncoupled lasers with respect to the average frequency. Basic solutions of (2) are called *compound laser modes (CLMs)* and are of the form

$$\begin{aligned} E_1(t) &= R_1 e^{i\omega t}, \quad N_1(t) = N_1, \\ E_2(t) &= R_2 e^{i\omega t+i\sigma}, \quad N_2(t) = N_2, \end{aligned} \tag{3}$$

where ω, σ, R_j, and N_j are all real-valued, and $R_j > 0$ for $j = 1, 2$.

Notice that if $\Delta = 0$ in (2), then the resulting system has an additional $\mathbf{Z}_2$ symmetry. That is, interchanging the two lasers gives the same system of equations. As noted in Erzgraber et al. (2006), this special case is important because it organizes the dynamics for small nonzero detuning.

Our results show that the symmetry structure of the system can be utilized to organize the manner that we seek CLMs, and to identify symmetry-breaking steady-state and Hopf bifurcations. Moreover, the later allows us to predict the symmetry group of the bifurcating branch of solutions from a symmetry-breaking bifurcation. For the rest of the paper, we only consider this symmetric two-laser system. While Erzgraber et al. (2006) analyzed the symmetric system through numerical bifurcation analysis, we employ a group-theoretic approach to provide additional classification on steady-state and Hopf bifurcations. Furthermore, for larger symmetric laser networks the presence of eigenvalues with higher multiplicity could post difficulties in implementing numerical bifurcation analysis. The usefulness of our method then becomes more apparent in these cases.

Before discussing the symmetric two-laser system, we first give some background material on delay differential equations. We present simple examples

that point out differences and similarities between *ordinary* differential equations (ODEs) and *delay* differential equation (DDEs).

BACKGROUND ON DDEs

Recall that the scalar ODE $\dot{x}(t) = -x(t)$ has the trivial solution $x(t) = 0$ as its only steady-state or equilibrium solution. If we try to seek solutions of the form $x(t) = x(0)e^{\lambda t}$, then substituting this ansatz to the ODE gives the characteristic equation $\lambda + 1 = 0$ which is a polynomial equation and hence has a finite number of roots. The stability of the trivial equilibrium solution requires that all roots of the characteristic equation to have negative real parts. Since the characteristic equation has only one root $\lambda = -1$, the trivial equilibrium solution is locally stable. Indeed, $x(0)e^{-t} \to 0$ as t increases without bound. If we modify the above ODE example to include a constant delay $\tau > 0$, then we obtain the DDE

$$\dot{x}(t) = -x(t-\tau).$$

To have a unique solution for $t > 0$, we need an initial history function $\phi(t)$ that belongs to the set of continuous functions mapping the delay interval $[-\tau, 0]$ to the set of real numbers $\Re$. For simplicity, we take this continuous function to be the constant function $\phi(t) = x(0)$ for $t \in [-\tau, 0]$. The above DDE also has the trivial solution $x(t) = 0$ as its only equilibrium solution. If we try to seek solutions of the form $x(t) = x(0)e^{\lambda t}$, then substituting this ansatz to the DDE gives the characteristic equation $\lambda + e^{-\lambda\tau} = 0$ which is a transcendental equation that is known to have an infinite number of roots. Similar to ODEs, the stability of the trivial equilibrium solution requires that all roots of the transcendental characteristic equation to have negative real parts. The trivial solution is in fact locally asymptotically stable for $\tau < \pi/2$ and is unstable for $\tau > \pi/2$. A proof of this result is given in Smith (2011).

We may view the above DDE as a perturbation of our ODE example. Hence, for small delay value, the solution to the DDE should be 'similar' to the solution of the ODE, which is the exponential function. As we increase τ, the solution to the DDE starts to oscillate, and for large enough delay value these oscillations grow in amplitude. Hopf bifurcation or the emergence of a periodic orbit occurs when we have a simple pair of purely imaginary eigenvalues, say $\lambda = \pm i\omega$ with $\omega > 0$. If we substitute $\lambda = i\omega$ to the transcendental characteristic equation $\lambda + e^{-\lambda\tau} = 0$ and then separate the real and imaginary parts, we get $\omega - \sin\omega\tau = 0$ and $\cos\omega\tau = 0$. This gives $\omega = 1$ using the Pythagorean trigonometric identity, and consequently $\tau = \pi/2$. This means that if we choose the delay value $\tau = \pi/2$, then the solution to the DDE will have regular oscillations.

The above example illustrates that delay causes oscillation of solutions, and thus Hopf bifurcation is not uncommon in system of DDEs. The reader may refer to Smith (2011) for detailed introduction to DDEs and its applications, and to Hale and Verduyn Lunel (1993) and Diekmann et al. (1995) for a more advanced treatment of DDEs.

SYMMETRIC TWO-LASER SYSTEM

We now consider the symmetric two-laser system described by the following LK rate equations:

$$\begin{aligned}
\dot{E}_1(t) &= (1+i\alpha)N_1(t)E_1(t)+\kappa e^{-iC_p}E_2(t-\tau),\\
\dot{E}_2(t) &= (1+i\alpha)N_2(t)E_2(t)+\kappa e^{-iC_p}E_1(t-\tau),\\
T\dot{N}_1(t) &= P-N_1(t)-(1+2N_1(t))\,|E_1(t)|^2,\\
T\dot{N}_2(t) &= P-N_2(t)-(1+2N_2(t))\,|E_2(t)|^2.
\end{aligned} \tag{4}$$

We claim that the above system (4) has symmetry group $\mathbf{Z}_2 \times \mathbf{S}^1$. To see this, let us first define the action of the groups $\mathbf{Z}_2 = \langle\gamma\rangle$ and the circle group $\mathbf{S}^1$, with elements ϑ, to the state variables $(E, N) := (E_1(t), E_2(t), N_1(t), N_2(t))$ as follows:

$$\begin{aligned}
\gamma\cdot(E,N) &= (E_2(t),E_1(t),N_2(t),N_1(t)),\\
\vartheta\cdot(E,N) &= (E_1(t)e^{i\vartheta},E_2(t)e^{i\vartheta},N_1(t),N_2(t)).
\end{aligned} \tag{5}$$

Observe that the order-two element γ of $\mathbf{Z}_2$ interchanges the two lasers, while the element ϑ of $\mathbf{S}^1$ acts only on the complex optical field $E_j(t)$ for $j = 1, 2$. The equivariance of (4) under $\mathbf{Z}_2 \times \mathbf{S}^1$ follows from the fact that if (E, N) is a solution to (4) then so are $\gamma \cdot (E, N)$ and $\vartheta \cdot (E, N)$.

Since system (4) has symmetry group $\mathbf{Z}_2 \times \mathbf{S}^1$, we expect its solutions to have the same symmetry group or a symmetry group that is a subgroup of $\mathbf{Z}_2 \times \mathbf{S}^1$. That is, we are interested with CLMs whose symmetry group are isotropy subgroups of $\mathbf{Z}_2 \times \mathbf{S}^1$. We first give the following definition and result from Golubitsky et al. (1988).

Definition. Let H be a subgroup of $\mathbf{\Gamma}$ and let $\vartheta: H \to S^1$ be a group homomorphism. We call

$$H^\vartheta = \{(h, \vartheta(h)) \in \Gamma \times \mathbf{S}^1 \mid h \in H\}$$

a twisted subgroup of $\mathbf{\Gamma} \times \mathbf{S}^1$.

In Golubitsky et al. (1988), it was shown that all proper isotropy subgroups of $\mathbf{\Gamma} \times \mathbf{S}^1$ are twisted subgroups. This result was also obtained in Collera (2012) specifically for $\mathbf{\Gamma} = \mathbf{Z}_n$, allowing us to find isotropy subgroups of $\mathbf{Z}_2 \times \mathbf{S}^1$. Table 1 enumerates the homomorphisms used to obtain the twisted subgroups of $\mathbf{Z}_2 \times \mathbf{S}^1$ which in turn, in this case, give the isotropy subgroups of $\mathbf{Z}_2 \times \mathbf{S}^1$.

The subgroups $\mathbf{Z}_2(\gamma)$ and $\mathbf{Z}_2(\gamma, \pi)$ of $\mathbf{Z}_2 \times \mathbf{S}^1$ are generated by the elements $(\gamma, 0)$ and (γ, π) of $\mathbf{Z}_2 \times \mathbf{S}^1$, respectively, and are both isomorphic to $\mathbf{Z}_2$. These isotropy subgroups can be organized in a lattice structure as shown in Figure 1, which will be relevant later on when we discuss symmetry-breaking bifurcations. The diagram

TABLE 1. Isotropy subgroups of $\mathbf{Z}_2 \times \mathbf{S}^1$.

Case	H	Homomorphism	Isotropy Subgroup
1	$\mathbf{Z}_2$	$\vartheta_1 : \gamma \mid\!\to 0$	$\mathbf{Z}_2(\gamma) = \langle(\gamma, 0)\rangle$
2	$\mathbf{Z}_2$	$\vartheta_2 : \gamma \mid\!\to \pi$	$\mathbf{Z}_2(\gamma, \pi) = \langle(\gamma, \pi)\rangle$

basically tells us what symmetry group should be expected on a bifurcating branch of solutions emanating from a symmetry-breaking bifurcation. Note that this method of finding isotropy subgroups of $\mathbf{Z}_2 \times \mathbf{S}^1$ can be adopted for larger laser systems and with different coupling types. For example, unidirectional, bidirectional, and all-to-all coupling types result to symmetry groups $\mathbf{Z}_n \times \mathbf{S}^1$, $\mathbf{D}_n \times \mathbf{S}^1$, and $\mathbf{S}_n \times \mathbf{S}^1$, respectively. The isotropy subgroup lattice then becomes more useful when dealing with larger symmetry groups.

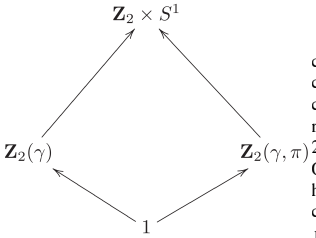

Figure 1. Subgroup lattice for $\mathbf{Z}_2 \times \mathbf{S}^1$.

Each isotropy subgroup fixes a certain form of CLM and as a consequence, in this case, we get constant values for the phase shift σ and relations on values of R_j and N_j for $j = 1, 2$. These are summarized in Table 2. Observe that for Case 1 and Case 2, we have $R_1 = R_2$ and $N_1 = N_2$. We take these common values to be R and N, respectively. Moreover, we call the CLMs corresponding to Case 1 given by

$$\begin{aligned}
E_j(t) &= Re^{i\omega t},\\
N_j(t) &= N,
\end{aligned} \tag{6}$$

for $j = 1, 2$, as the *fully symmetric CLMs*. These CLMs have symmetry group $\mathbf{Z}_2(\gamma)$. The relations given in the last column of Table 2 will be used in the next section in our search for symmetric CLMs.

TABLE 2. CLMs fixed by isotropy subgroups of $\mathbf{Z}_2 \times \mathbf{S}^1$.

Subgroup	CLMs Fixed	Relations
$\mathbf{Z}_2(\gamma)$	$(E_1(t), E_1(t), N_1(t), N_1(t))$	$\sigma = 0, R_1 = R_2, N_1 = N_2$
$\mathbf{Z}_2(\gamma, \pi)$	$(E_1(t), -E_1(t), N_1(t), N_1(t))$	$\sigma = \pi, R_1 = R_2, N_1 = N_2$

SYMMETRIC CLMs

To find symmetric CLMs, that is, CLMs fixed by the isotropy subgroups of $\mathbf{Z}_2 \times \mathbf{S}^1$, we substitute the ansatz in (3) to the equations in (4) and then split each of the first two equations in (4) into real and imaginary parts. We obtain six equations with unknowns $\omega, \sigma, R_1, R_2, N_1$, and N_2. We then eliminate N_1 and N_2 from the first 2 pairs of equations, giving us the two equations

$$\omega = -\frac{R_2}{R_1}\kappa\sqrt{1+\alpha^2}\,\sin(C_p+\omega\tau+\arctan\alpha\mp\sigma) \tag{7}$$

after using the identity $\alpha\cos\theta + \sin\theta = \sqrt{1+\alpha^2}\sin(\theta + \arctan\alpha)$ for $\alpha \geq 0$. Since $R_1 = R_2$, both for Case 1 and Case 2, the equations in (7) become

$$\omega = \mp\kappa\sqrt{1+\alpha^2}\,\sin(C_p+\omega\tau+\arctan\alpha) \tag{8}$$

respectively for Case 1 with $\sigma = 0$, and for Case 2 with $\sigma = \pi$. We summarize the above discussion in the following theorem.

Theorem 1. For the two-laser system in (4), symmetric CLMs can be found by solving for ω in the transcendental equation

$$\omega+\kappa\sqrt{1+\alpha^2}\,\sin(C_p+\omega\tau+\arctan\alpha+\sigma)=0 \tag{9}$$

for each of the two cases $\sigma = 0$ and $\sigma = \pi$.

Equation (9) will always have at least one solution in ω since it can be viewed as finding the intersections of a diagonal line and a sine wave. Once an ω-value is known, we can then solve for N_1 and N_2, and then use these values to solve for R_1 and R_2. For both Case 1 and Case 2, these values are given by

$$N_j = \frac{\omega}{\alpha+\tan(C_p+\omega\tau)} \quad \text{and} \quad R_j = \sqrt{\frac{P-N_j}{1+2N_j}}$$

for $j = 1, 2$. The set of values $(\omega, \sigma, R_1, R_2, N_1, N_2)$ corresponds to a CLM in (3). We note that computations leading to the transcendental equations in (8) were also done in Erzgraber et al (2006) for the general case when the detuning Δ in (2) is nonzero. Here, we focus mainly in using the isotropy subgroups in deriving the transcendental equations as this technique organizes the manner we seek symmetric CLMs, and can be generalized for larger symmetric laser networks.

We now find symmetric CLMs of system (4). We adopt the following physically meaningful parameter values used in Erzgraber et al. (2006):

$$\alpha = 2.5,\ T = 392,\ P = 0.23,\ \tau = 20,\ \kappa = 0.1, \text{ and } C_p = -\pi,$$

and then solve for ω in (9) with $\sigma = 0$ numerically. The obtained values of ω and their corresponding R and N values are summarized in Table 3. Once a CLM is known, we can then continue or follow it into a branch of CLMs by varying a single parameter. Stability and bifurcations along this branch of CLMs can also be determined using DDE-Biftool (Engelborghs et al. 2001), which is a Matlab package for numerical continuation and bifurcation analysis of delay differential equations (DDEs).

TABLE 3. Values obtained from solving the transcendental equation (9) with $\sigma = 0$. Each set of values (ω, N, R) represents a CLM.

ω	N	R
-0.179987	-0.089687	0.624151
-0.073299	0.010460	0.463724
0.082077	-0.007069	0.490376

In the paragraph that follows, we summarize the numerical continuation and numerical bifurcation analysis implemented by Erzgraber et al. (2006) for system (4). We then point out that a process of identifying symmetry-breaking bifurcations can be carried out using a group-theoretic approach that will complement and corroborate the numerical results in Erzgraber et al. (2006).

The idea is to start with a given CLM and then follow it as an equilibrium solution in DDE-Biftool by varying the coupling phase parameter C_p to obtain a branch of CLMs. This parameter choice has the advantage that values of C_p only need to cover an interval of length at least 2π since the symmetric two-laser system (4) has a 2π-translational symmetry in C_p. Moreover, the coupling phase C_p can be changed accurately in experiments (Agrawal and Dutta 1986). The branch of CLMs obtained in DDE-Biftool, using the CLM in Table 3 with $\omega = -0.179987$ as our 'starting point', is shown in Figure 2A. The three dots correspond to the three CLMs given in Table 3. Observe further that in the ωN-plane, the 2π-translational symmetry in C_p is hidden. Figure 2B shows the same branch of CLMs (thick line), but this time in the C_pN-plane where the 2π-translational symmetry in C_p is evident. A second curve (thin line) is also shown, and this corresponds to Case 2 with $\sigma = \pi$. To summarize, the two curves shown in Figure 2B correspond to Case 1 (thick line) and Case 2 (thin line). These are the same curves but are π-translated to each other. In ωN-plane, these two curves overlap, and thus only one curve is shown in Figure 2A. Erzgraber et al. (2006) also used DDE-Biftool to determine branch stability, and locate steady-state and Hopf bifurcation points along branches of CLMs. In Figure 2C, stable and unstable parts of the branch of CLMs are shown in green and magenta, respectively. Steady-state and Hopf bifurcations are marked with (+) and (○), respectively. We note that the two branches in Figure 2D, plotted in the C_pN-plane, are exactly the same in terms of stability and bifurcations but are π-translated with each other.

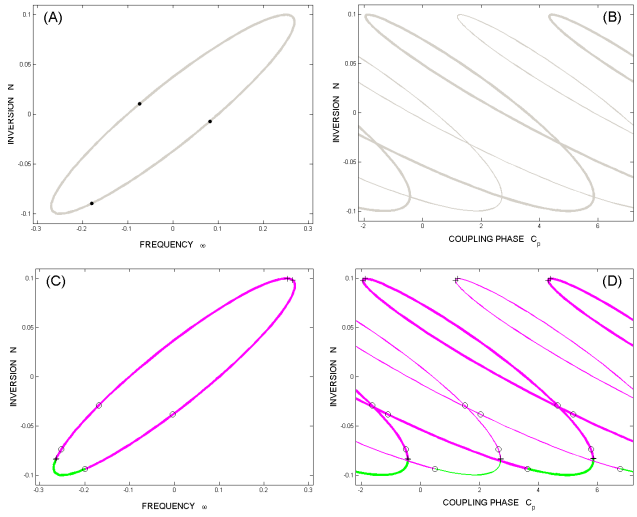

Figure 2. (A) A branch of CLMs, in ωN-plane, obtained using DDE-Biftool by following the CLMs in Table 3. (B) Branches of CLMs, in C_pN-plane, for Case 1 (thick line) and Case 2 (thin line). (C and D) Stability information and bifurcations are obtained using DDE-Biftool. Green indicates the stable part of the branch while the unstable part is shown in magenta. The symbols (+) and (○) indicate steady-state and Hopf bifurcations, respectively.

DDE-Biftool was able to locate steady-state and Hopf bifurcations along branches of CLMs. However, there is no further classification on these bifurcations into regular or symmetry-breaking. Knowledge of this classification allows one to predict the symmetry group of bifurcating branches of solutions from these bifurcation points. We now give a method that utilizes the symmetry structure of system (4) to explicitly locate steady-state and Hopf bifurcations, that is, without using DDE-Biftool. Furthermore, this group-theoretic approach provides us with the above mentioned classification.

SYMMETRY-BREAKING BIFURCATIONS

Symmetry plays an important role in our study, as the action of a symmetry group decomposes the physical space into isotypic components. This decomposition then allows us to write the characteristic matrix into a block-diagonal form. This technique gives us a means of locating steady-state and Hopf bifurcations explicitly, that is, without using DDE-Biftool. Moreover, a classification of these bifurcations into regular or symmetry-breaking is given based on which diagonal block the critical eigenvalue came from.

This section is organized as follows. First, we derive the characteristic equation corresponding to the linear variational equation around the fully symmetric CLM (6). Next, we use the isotypic decomposition of the physical space to write the characteristic matrix into a block diagonal form. Lastly, we find steady-state and Hopf bifurcations, and classify them into regular or symmetry-breaking.

Linear Variational Equation around a CLM

We first write the symmetric two-laser system (4) in polar coordinates. We let $E_j(t) = R_j(t)\, e^{i\varphi_j(t)}$, for $j = 1, 2$, so that the rate equations for the j^{th} laser become

$$\begin{aligned}
\dot{R}_j(t) &= N_j(t)R_j(t) + \kappa R_k(t-\tau)\cos(-C_p + \varphi_k(t-\tau) - \varphi_j(t)),\\
\dot{\varphi}_j(t) &= \alpha N_j(t) + \kappa \frac{R_k(t-\tau)}{R_j(t)}\sin(-C_p + \varphi_k(t-\tau) - \varphi_j(t)),\\
\dot{N}_j(t) &= \frac{1}{T}\left[P - N_j(t) - (1+2N_j(t))\,|R_j(t)|^2\right],
\end{aligned} \tag{10}$$

for $j = 1, 2$, and $k = 1, 2$ with $k \neq j$. If we let $X_j(t) = [R_j(t), \phi_j(t), N_j(t)]^T$ and $Y_j(t) = X_j(t-\tau)$ then (10) can be written in a form $\dot{X}_j(t) = f(X_j(t), Y_k(t))$ for $j = 1, 2$, and $k = 1, 2$ with $k \neq j$. Our aim is to obtain the linear variational equation around the fully symmetric CLM (6). We first compute for

$$\overline{A} := d_{X_j(t)} f(CLM) \quad \text{and} \quad \overline{B} := d_{Y_j(t)} f(CLM),$$

where both quantities are evaluated at the fully symmetric CLM (6). We get

$$\overline{A} = \begin{bmatrix} -c & -Rs & R \\ s/R & -c & \alpha \\ -C_2 & 0 & -C_1 \end{bmatrix} \quad \text{and} \quad \overline{B} = \begin{bmatrix} c & Rs & 0 \\ -s/R & c & 0 \\ 0 & 0 & 0 \end{bmatrix},$$

where

$$s = \kappa \sin(C_p + \omega\tau), \quad C_1 = \frac{1}{T}(1+2R^2),$$

$$c = \kappa \cos(C_p + \omega\tau), \quad C_2 = \frac{2}{T}(1+2N)R,$$

and using the identity $N = -c$ obtained from the first equation of (10). Now, let

$$M_1 = \begin{bmatrix} \overline{A} & 0 \\ 0 & \overline{A} \end{bmatrix} \quad \text{and} \quad M_2 = \begin{bmatrix} 0 & \overline{B} \\ \overline{B} & 0 \end{bmatrix}.$$

Then, the linear variational equation around the fully symmetric CLM (6) is given by $\dot{X}(t) = M_1 X(t) + M_2 X(t-\tau)$, whose corresponding characteristic equation is $\det \Delta(\lambda) = 0$ where $\Delta(\lambda) = \lambda I_6 - M_1 - e^{-\lambda\tau} M_2$. A similar computation as above in obtaining the linear variational equation around a CLM was also done in Verduyn Lunel and Krauskopf (2000) for the case of one-laser model. Notice that if we let $A = \lambda I_3 - \overline{A}$ and $B = -e^{-\lambda\tau}\overline{B}$, then

$$L := \Delta(\lambda) = \begin{bmatrix} A & B \\ B & A \end{bmatrix} \tag{11}$$

where blocks A and B are 3×3 matrices.

Isotypic Decomposition

We now transform L into a block-diagonal form using a technique from Golubitsky et al. (1988). The symmetry group of the fully symmetric CLM (6) is $\mathbf{Z}_2(\gamma)$. We define the action of $\mathbf{Z}_2(\gamma)$ on the two-dimensional Euclidean space $\Re^2$ by

$$\gamma \cdot \begin{bmatrix} x \\ y \end{bmatrix} = \begin{bmatrix} y \\ x \end{bmatrix},$$

where $x, y \in \Re$. Observe that the subspaces T and A of $\Re^2$, given by

$$T = \left\{ \begin{bmatrix} v \\ v \end{bmatrix}, v \in \Re \right\} \quad \text{and} \quad A = \left\{ \begin{bmatrix} -v \\ v \end{bmatrix}, v \in \Re \right\},$$

are invariant under $\mathbf{Z}_2(\gamma)$. Also, note that $\mathbf{Z}_2(\gamma)$ acts trivially on T, and non-trivially on A. The subspace A is an orthogonal complement of T. Both T and A are one-dimensional, and thus irreducible. This $\mathbf{Z}_2(\gamma)$-action decomposes $\Re^2$ into $T \oplus A$, where $\mathbf{Z}_2(\gamma)$ acts on T by the trivial representation, and on A by the alternating representation.

We claim that the physical space $\Re^6$, for the two-laser system (4), has the isotypic decomposition $\Re^6 = T^3 \oplus A^3$ under the action of $\mathbf{Z}_2(\gamma)$. To see this, consider the subspaces V_0 and V_1 of $\Re^6$ whose respective elements are of the form

$$v_0 = \begin{bmatrix} v \\ v \end{bmatrix} \quad \text{and} \quad v_1 = \begin{bmatrix} -v \\ v \end{bmatrix}$$

where $v \in \Re^3$. We define the action of $\mathbf{Z}_2(\gamma)$ on $\Re^6$ as follows

$$\gamma \cdot \begin{bmatrix} w \\ z \end{bmatrix} = \begin{bmatrix} z \\ w \end{bmatrix}$$

where $w, z \in \Re^3$. Notice that both V_0 and V_1 are invariant subspaces under this action of $\mathbf{Z}_2(\gamma)$ on the physical space $\Re^6$. Also, $\mathbf{Z}_2(\gamma)$ acts trivially on V_0 and non-trivially on V_1, and V_1 is an orthogonal complement of V_0. Thus, $\mathbf{Z}_2(\gamma)$ acts on V_0 by three copies of the trivial action, and $\mathbf{Z}_2(\gamma)$ acts on V_1 by three copies of the non-trivial action. Since $\mathbf{Z}_2(\gamma)$ has only two distinct irreducible representations and the trivial one occurs only on V_0, we have $\Re^6 = T^3 \oplus A^3$.

We now use this isotypic decomposition of the physical space to transform the characteristic matrix L in (11) into a block-diagonal form. We first look at the action of L on the elements of the invariant subspaces V_0 and V_1. Notice that

$$Lv_0 = \begin{bmatrix} A & B \\ B & A \end{bmatrix}\begin{bmatrix} v \\ v \end{bmatrix} = \begin{bmatrix} (A+B)v \\ (A+B)v \end{bmatrix}, \quad \text{and} \quad Lv_1 = \begin{bmatrix} A & B \\ B & A \end{bmatrix}\begin{bmatrix} -v \\ v \end{bmatrix} = \begin{bmatrix} (A-B)(-v) \\ (A-B)v \end{bmatrix}.$$

The above equations imply that eigenvalues of $L\big|_{V_0}$ are those of $A + B$, and similarly, eigenvalues of $L\big|_{V_1}$ are those of $A - B$. The block $A + B$ corresponds to the action of L on $V_0 = T^3$, while the block $A - B$ corresponds to the action of L on $V_1 = A^3$. Hence, L can be written into the block-diagonal form

$$L = \Delta(\lambda) = \begin{bmatrix} A+B & 0 \\ 0 & A-B \end{bmatrix}. \tag{12}$$

We now use this block-diagonal form of L to find and classify steady-state and Hopf bifurcations.

Steady-State Bifurcations

Steady-state bifurcation happens when we have an eigenvalue $\lambda = 0$. Our task now is to find values of the coupling phase parameter C_p where steady-state bifurcation occurs, that is, when det $\Delta(\lambda)\,|_{\lambda=0} = 0$. From (12), we only need to consider the equations det $(A \pm B)\,|_{\lambda=0} = 0$. Recall that $A = \lambda I_3 - \overline{A}$ and $B = -e^{-\lambda\tau}\overline{B}$ Thus,

$$A \pm B = \begin{bmatrix} \lambda + c(1 \mp e^{-\lambda\tau}) & Rs(1 \mp e^{-\lambda\tau}) & -R \\ -\dfrac{s}{R}(1 \mp e^{-\lambda\tau}) & \lambda + c(1 \mp e^{-\lambda\tau}) & -\alpha \\ C_2 & 0 & \lambda - C_1 \end{bmatrix}. \tag{13}$$

The diagonal block $A - B$ corresponds to the action of L on V_1, and $\mathbf{Z}_2(\gamma)$ acts on the invariant subspace $V_1 = A^3$ by three copies of the alternating representation. With this order-two symmetry, we expect pitchfork bifurcations to occur (Chossat and Lauterbach 2006). To find these bifurcation points, we look for the intersections, modulo 2π in C_p, of the curves corresponding to the transcendental equation in (9) with $\sigma = 0$, and det $(A - B)\,|_{\lambda=0} = 0$. The former gives us the branch of CLMs with symmetry group $\mathbf{Z}_2(\gamma)$, while the latter gives us the pitchfork bifurcation points along this branch of CLMs. The left panel of Figure 3 shows these two curves. Observe that the intersections, modulo 2π, happen exactly on two points marked with (+). Recall that the points with marker (+) are the steady-state bifurcation points obtained numerically in DDE-Biftool. The only difference here is that we have a further classification of these steady-state bifurcations into symmetry-breaking bifurcations, which in this case are pitchfork bifurcations.

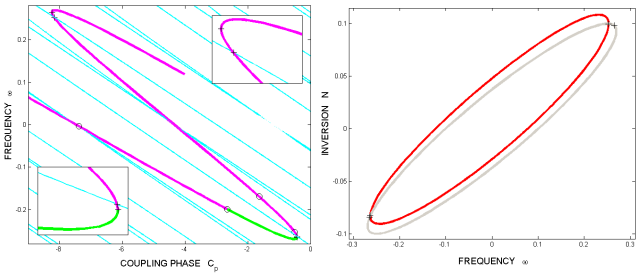

Figure 3. (Left) Pitchfork bifurcations are identified by looking at the intersections of the branch of CLMs and the cyan curve corresponding to det$(A - B)\,|_{\lambda=0} = 0$. (Right) Following a pitchfork bifurcation in DDE-Biftool reveals a new branch of CLMs (red ellipse).

The right panel of Figure 3 shows a bifurcating branch of CLMs (red ellipse) emanating from the pitchfork bifurcations that we have identified earlier. This bifurcating branch of CLMs was obtained in DDE-Biftool by following either of the two pitchfork bifurcation points. The subgroup lattice in Figure 1 shows the possible symmetry group of a bifurcating branch of CLMs from a symmetry-breaking bifurcation. On the original branch of CLMs, we have $E_1(t) = E_2(t)$ and $N_1(t) = N_2(t)$, while on the bifurcating branch of CLMs, we have $E_1(t) \neq E_2(t)$ and $N_1(t) \neq N_2(t)$. The bifurcation here breaks the symmetry from $\mathbf{Z}_2(\gamma)$ of the original branch into just the identity $\mathbf{1}$ of the bifurcating branch of CLMs.

Hopf Bifurcations

We now focus our attention to Hopf bifurcations. This type of bifurcation happens when we have a simple conjugate pair of purely imaginary eigenvalues, say $\lambda = \pm i\beta$ with $\beta > 0$. Our goal is to find values of the coupling phase parameter C_p where Hopf bifurcations occur. To do this, we employ the same technique as in the previous section in finding steady-state bifurcations. That is, we look for the intersections of the curve corresponding to the transcendental equation in (9) with $\sigma = 0$ to each of the curve with corresponding equations det$(A + B)\,|_{\lambda=i\beta} = 0$ and det$(A - B)\,|_{\lambda=i\beta} = 0$. Regular Hopf bifurcations and symmetry-breaking Hopf bifurcations are then identified depending on which diagonal block the eigenvalues came from. Notice that we can solve for C_p in (9) with $\sigma = 0$, and obtain

$$C_p = \arcsin\left(\frac{-\omega}{\kappa\sqrt{1+\alpha^2}}\right) - \omega\tau - \arctan\alpha, \tag{14}$$

$$C_p = \pi - \arcsin\left(\frac{-\omega}{\kappa\sqrt{1+\alpha^2}}\right) - \omega\tau - \arctan\alpha. \tag{15}$$

We get the expression in (15) using the identity $\sin(\pi - x) = \sin(x)$.

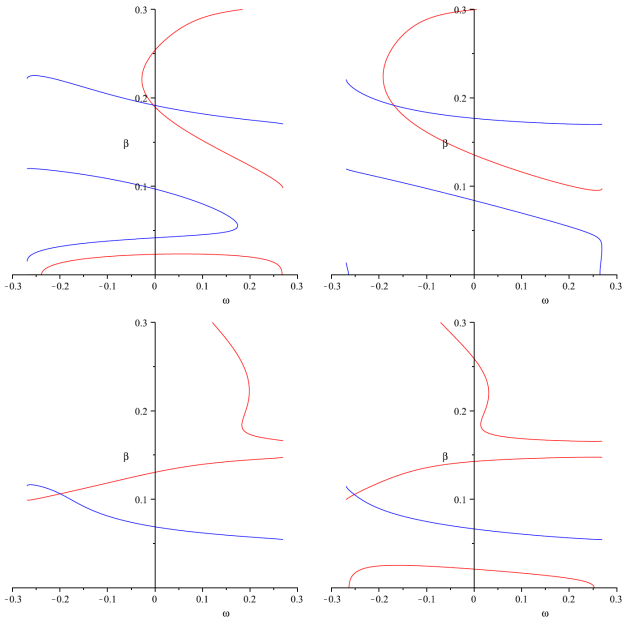

Figure 4. (Top Row) Regular Hopf bifurcations are obtained by looking at the intersections of the real part (red) and imaginary part (blue) of det$(A + B)\,|_{\lambda=i\beta} = 0$. (Bottom Row) Symmetry-breaking Hopf bifurcations are obtained by looking at the intersections of the real part (red) and imaginary part (blue) of det$(A - B)\,|_{\lambda=i\beta} = 0$. The left and right panels of each row use values of C_p in (14) and (15), respectively.

Regular Hopf bifurcations are obtained from the diagonal block $A + B$. In the top row of Figure 4, we look at the intersections of the real part (red curve) and imaginary part (blue curve) of det$(A + B)\,|_{\lambda=i\beta} = 0$. The figure in the top left panel uses values of C_p in (14) while the figure in the top right panel uses values of C_p in (15). Similarly, symmetry-breaking Hopf bifurcations are obtained from the diagonal block $A - B$. The bottom row of Figure 4 shows the intersections of the real part (red curve) and imaginary part (blue curve) of det$(A - B)\,|_{\lambda=i\beta} = 0$ where the figure in the bottom left panel uses values of C_p in (14) while the figure in the bottom right panel uses values of C_p in (15). In total, we have two regular Hopf bifurcations and two symmetry-breaking Hopf bifurcations. The required values of C_p are obtained using the ω values from the intersections of the curves in Figure 4.

We now illustrate the above classification of Hopf bifurcations using numerical continuation in DDE-Biftool. We follow all Hopf bifurcations to obtain corresponding branches of periodic solutions as shown in Figure 5. These branches of periodic solutions serve as 'bridges' between Hopf bifurcations. To be precise, it is worth mentioning that they connect Hopf bifurcations of the same type. That is, branches in blue connect a pair of regular Hopf bifurcations while branches in red connect symmetry-breaking Hopf bifurcations.

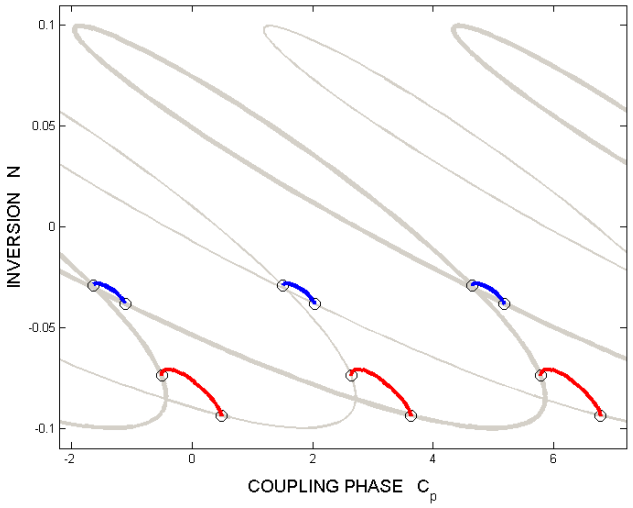

Figure 5. Branches of periodic solutions serve as 'bridges' between Hopf bifurcations. Branches in blue connect a pair of regular Hopf bifurcations while branches in red connect a pair of symmetry-breaking Hopf bifurcations.

We examine these branches of periodic solutions further by looking at the behavior of each laser. In Figure 6, we plot the inversions $N_1(t)$ and $N_2(t)$. The left column corresponds to the branch of periodic solutions that connects two regular Hopf bifurcations. Here, both lasers are in phase with each other, and periodic solutions in this branch have spatio-temporal symmetry $\mathbf{Z}_2(\gamma)$. The right column of Figure 6 corresponds to the branch of periodic solutions connecting two symmetry-breaking Hopf bifurcations. The two lasers here are half a period out of phase with each other, and periodic solutions in this branch have spatio-temporal symmetry $\mathbf{Z}_2(\gamma, \pi)$. That is, interchanging the two lasers amounts to a displacement of half a period on each laser. The subgroup lattice in Figure 1, in fact, already predicted this scenario. That is, periodic solutions can only have the two isotropy subgroups as its symmetry group.

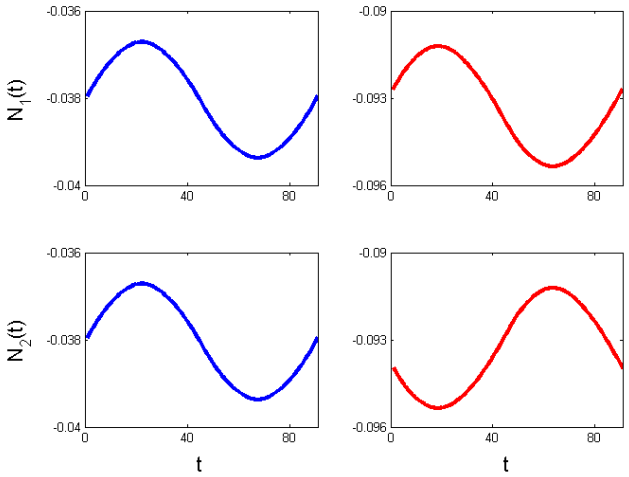

Figure 6. Periodic solutions that emanate from regular Hopf bifurcations (left column) are in phase while those that emerge from symmetry-breaking Hopf bifurcations (right column) are half a period out of phase.

CONCLUSION

The main contribution of this study is the classification of symmetry-breaking bifurcations using a group-theoretic approach. We show that the symmetry of a system plays an important role in studying the types of solutions and in classifying bifurcations arising in equivariant systems. Knowledge of this classification allows us to predict the behavior of a bifurcating branch of solutions that emanates from a symmetry-breaking bifurcation. We also note that the techniques used in this study, such as the derivation of the transcendental equations which is the key in finding symmetric solutions, and the isotypic decomposition of the physical space which allows us to identify symmetry-breaking steady-state and Hopf bifurcations, can be extended for laser systems with unidirectional, bidirectional, and all-to-all coupling types. Implementing a numerical bifurcation analysis in these larger symmetric laser networks could be tricky due to the presence of eigenvalues with higher multiplicity. The relevance of our group-theoretic approach then becomes more apparent in these cases.

ACKNOWLEDGEMENTS

The author acknowledges the assistance of Hartmut Erzgräber in using DDE-Biftool, and the support from University of the Philippines Baguio.

CONFLICTS OF INTEREST

There are no conflicts of interest in this study.

REFERENCES

Agrawal GP, Dutta NK. Long-wavelength semiconductor lasers. New York:Van Nostrand Reinhold, 1986.

Alsing PM, Kovanis V, Gavrielides A, Erneux T. Lang and Kobayashi phase equation. Phys Rev A 1996; 53:4429-4434.

Chossat P, Lauterbach R. Methods in equivariant bifurcation and dynamical systems. Singapore:World Scientific, 2000.

Collera JA. Bifurcations of periodic solutions of functional differential equations with spatio-temporal symmetries. PhD thesis, Queen's University, Kingston, 2012.

Diekmann O, van Gils SA, Verduyn Lunel SM, Walther H-O. Delay Equations: Functional-, Complex-, and Nonlinear Analysis, Springer, Berlin, 1995.

Engelborghs K, Luzyanina T, Samaey G. DDE-BIFTOOL v. 2.00 user manual: a matlab package for bifurcation analysis of delay differential equations. Technical report, Department of Computer Science, K. U. Leuven, Leuven, 2001.

Erzgraber H, Krauskopf B, Lenstra D. Compound laser modes of mutually delay-coupled lasers. SIAM J Appl Dyn Syst 2006; 5(1):30-65.

Golubitsky M, Stewart I, Schaeffer DG. Singularities and groups in bifurcation theory II. New York:Springer-Verlag,1988.

Hale JK, Verduyn Lunel SM. Introduction to Functional Differential Equations, Springer, New York, 1993.

Lang R, Kobayashi K. External optical feedback effects on semiconductor injection laser properties. IEEE J Quantum Electron 1980; 16(3):347-355.

Smith H. An Introduction to Delay Differential Equations with Sciences Applications. Springer, 2011.

Verduyn Lunel SM, Krauskopf B. The mathematics of delay equations with application to the Lang-Kobayashi equations. In: Krauskopf B, Lenstra D, eds. Fundamental Issues of Nonlinear Laser Dynamics. AIP Conf. Proc. volume 548. New York: American Institute of Physics, 2000:66-86.